CONVECTIVE FLOW BOILING

Proceedings of Convective Flow Boiling, An International Conference held at the Banff Center for Conferences, Banff, Alberta, Canada
April 30 – May 5, 1995

EDITOR
JOHN C. CHEN
LEHIGH UNIVERSITY
Bethlehem, Pennsylvania, USA

ASSOCIATE EDITORS
Yasunobu Fujita
Kyushi University
Fukuka, Japan

Franz Mayinger
Technical University of Munich
Germany

Ralph Nelson
Los Alamos National Laboratory
New Mexico, USA

Taylor & Francis
Publishers since 1798

USA	Publishing Office:	Taylor & Francis 1101 Vermont Avenue, NW Washington, DC 20005-3521 Tel: (202) 289-2174 Fax: (202) 289-3665
	Distribution Center:	Taylor & Francis 1900 Frost Road Suite 101 Bristol, PA 19007-1598 Tel: (215) 785-5800 Fax: (215) 785-5515
UK		Taylor & Francis Ltd. 1 Gunpowder Square London EC4A 3DE Tel: 0171 583 0490 Fax: 0171 583 0581

CONVECTIVE FLOW BOILING

1 2 3 4 5 6 7 8 9 0 B R B R 9 8 7 6

Printing and binding by Braun-Brumfield, Inc.

A CIP catalog record for this book is available from the British Library.
∞ The paper in this publication meets the requirements of the ANSI Standard Z39.48-1984 (Permanence of Paper)

Library of Congress Cataloging-in-Publication Data

International Conference on Convective Flow Boiling (1st : 1995 :
Banff, Atla.)
Convective flow boiling: proceedings of Convective Flow Boiling, an International Conference held at the Banff Center for Conferences, Banff, Alberta, Canada, April 30–May 5, 1995 / editor, John C. Chen; associate editors, Yasunobu Jukita . . . [et al.].
p. cm.
Includes index.
1. Heat—Transmission—Congresses. Ebullition—Congresses.
I. Chen, John C., date. II. Title.
TJ260.I574 1995
621.402'2—dc20 96-8655
ISBN 1-56032-507-0 (cloth) CIP

ADVANCED EXPERIMENTAL METHODS

Franz Mayinger
Lehrstuhl A für Thermodynamik
Technische Universität München
München, Germany

ABSTRACT

The enormous advances in electronic data processing today enable the engineer to formulate fluiddynamic transport processes, especially also with phase change in a detailed mathematical, numerical way, and modern date aquisition systems make it possible to gain detailed insight into the nature of physical phenomena.

Modern optical methods and also impedance methods are especially well suited for experimental studies, because of their inertialess and non-invasive mode of operation. Possible applications of optical methods, and also impedance methods are briefly described with emphasis to heat transfer with phase change and also to fluiddynamics in two-phase flow. The examples demonstrate the capabilities and the importance of new measuring techniques.

1. INTRODUCTION

Flow boiling heat transfer is going along with very dynamic processes like nucleation, bubble growth, bubble collapse, phase interface interactions and mixing between the phases. These processes result in thermo- and fluiddynamic conditions, responsible for heat transfer and friction-loss for example. To improve mathematical modelling of transport processes, it is essential to know details of phase interactions as good as possible. A key for such insights are advanced experimental techniques, which work non-invasive and inertialess. Optical methods offer several possibilities to get a better knowledge of thermo-, fluiddynamic events in convective flow boiling.

However also non-optical methods like sensors, working on a capacitive basis, experienced a very remarkable development with respect to non-invasivity and signal forming of low inertia. Methods, based on the attenuation of ionising rays like X-rays or Gamma-rays do not interfere with the boiling flow also, however, they need a certain counting rate, which means, that they do not work inertialess.

The development of optical methods and also of capacitive techniques was supported by the availability of new electronic devices, which allow to reduce the data processing considerably, having been very time consuming in the past. So modern electronics, together with newly developed computer software, opened new prospects for optical techniques, applicable to convective flow boiling.

There are several examples for modern optical measuring techniques generally being of interest in heat- and mass transfer and in fluid-dynamics (Mayinger, 1994). These techniques are using various physical effects and find a broad field of applications. They are either working on a global basis or give only pointwise information. In heat- and mass transfer mainly temperature, concentration and velocity are of interest. For each physical property usually various optical techniques can be applied. Velocity in a droplet-spray for example can be measured by pulsed laser holography (global method) or by laser doppler anemometry (pointwise technique, LDA or PDA).

Holographic interferometry allows to determine the temperature field and by this gives precise data for evaluating heat transfer.

In addition one has to mention Particle Image-Velocimetry, which is mainly using light sheet illumination and which is competitive to double- or multi-pulse-holography.It is not possible to discuss all optical techniques known from the literature in detail here, and therefore emphasis is given to

- Holography
- Holographic Interferometry and
- Laser-Induced Fluorescence

In the field of non-optical techniques a brief discussion will be devoted to a non-invasive technique of the capacitive method, based on the dielectric constant of liquid and vapour. Examples of application will demonstrate the usefulness and the capability of these methods. Brief comments will also be given on computer-aided evaluation of the optical signals or the optical images.

2. HOLOGRAPHY

The general theory of holography is so comprehensive, that for a detailed description one must refer to the literature (Gabor 1951, Kiemle, Röss 1969, Mayinger 1994). Here only the principles, necessary for understanding the holographic measurement technique can be mentioned. In Fig. 1 the holographic 2-step image forming process of recording and reconstructing an arbitrary wave front is illustrated. The object is illuminated by a monochromatic light source and the reflected, scattered light falls directly onto a holographic plate. This object wave has a very complicated wave front. According to the principle of Huygens, one however can regard it to be the super-position of many elementary spherical waves. In order to simplify the matter, only one wave is drawn in Fig. 1. This wave is superimposed by a second one called reference wave. If both waves are mutually coherent, they will form a stable interference pattern, when they meet on a photographic plate. This system of fringes can therefore be recorded on a photographic emulsion. After the development, the plate is called "Hologram". The microscopic pattern (in general it consists of up to 3000 lines per mm) contains all information about the wave. The amplitude is recorded in the form of different contrast of the fringes, the phase is recorded in the spatial variations of the pattern.

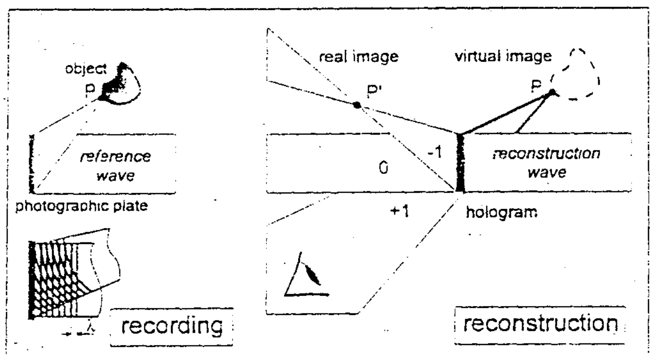

Figure 1. Principle of Holographic Two-Step Image-Forming Process.

If the plate, after chemical processing, is illuminated by a light beam, similar to the original reference-wave, the microscopic pattern acts like a diffraction grating with variable grating constant. The light transmitted, consists of a zero-order wave, travelling in the direction of the reconstructing beam, plus 2 first-order waves. One of these first-order waves travels in the same direction as the original object wave and has the same amplitude and phase distribution. This first-order wave produces a virtual image in front of the holographic plate, seen from the side of the incoming reference beam. The other wave goes in the opposite direction and creates a real image of the object behind the photographic plate. This real image can be studied with various reconstruction devices, such as a microscope.

For conventional application of holography one can use laser emitting continuous light. The recording of very fast moving or changing objects - like in convective, two-phase flow - needs ultra-short exposure times, which can be achieved by using a pulsed laser, for example a ruby-laser with pulse durations of 20 - 30 ns. A holographic set-up, using a pulsed laser is shown in Fig. 2.

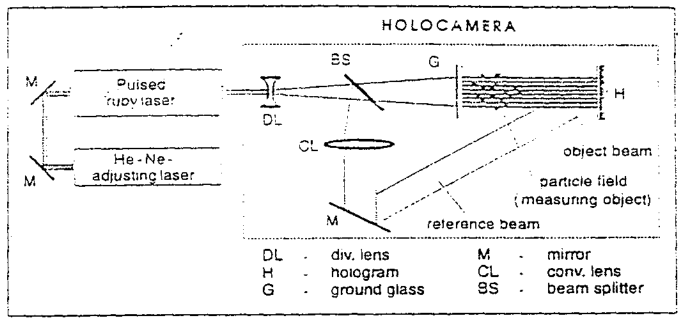

Figure 2. Holographic Set-Up for Ultra-Short Time Exposures with a Pulsed Laser.

A more sophisticated arrangement for recording pulsed laser holograms is presented by Fig. 3. In this arrangement the light, emitted by the pulsed ruby-laser, travels through a lense- and mirror system, where it is expanded, devided and guided through the measuring object and onto the holographic plate. This set-up is suitable for studying particle flow or phase distribution in multi-phase mixtures. It allows to visualise dispersed flow - like in post dry-out heat transfer with droplets not smaller than 10λ, whereby λ is the wave-length of the laser light.

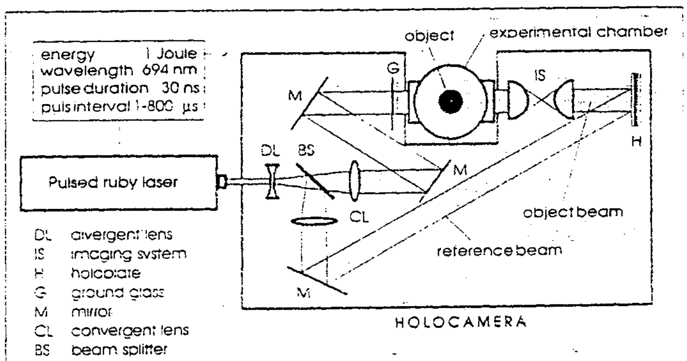

Figure. 3: Holographic Interferometer for Spray Analysis.

If the electronic system of the ruby-laser allows to emit more than one laser pulse within a very short period of time, sequences of the droplet- or spray-behaviour can be stored on the photographic emulsion of the same holographic plate, from which the velocity of the droplets, as well as their changes in size and geometric form can be evaluated. The evaluation however needs a very sophisticated and computerised procedure.

For evaluating the hologram, it first has to be reconstructed, as demonstrated in Fig. 4. After chemical processing the holographic plate is replaced in the old position and then illuminated by a continuously light-emitting helium-neon laser. If the holographic plate is replaced in the same orientation as during the recording process, one can look at it with the naked eye and one sees a virtual image of the droplet cloud or spray, exactly at the place where it was produced previously. For a quantitative evaluation one needs a closer examination via an enlarging lense or a microscope, which for example is connected with a video-camera. To do this, the holographic plate has to be turned by 180°, when positioning it to the old place. This is demonstrated in the lower part of Fig. 4. By illuminating with the reconstruction beam, a real image of the spray or droplet cloud is now produced, which has a three-dimensional extension.

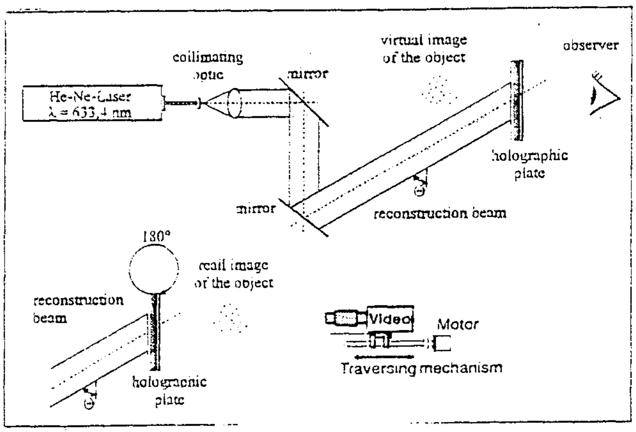

Figure 4. Optical Arrangement for the Reconstruction of Pulsed Laser Holograms.

An example of the arrangement of the video-camera, together with the evaluating components - computer, digitizer and monitor - is shown in Fig. 5.

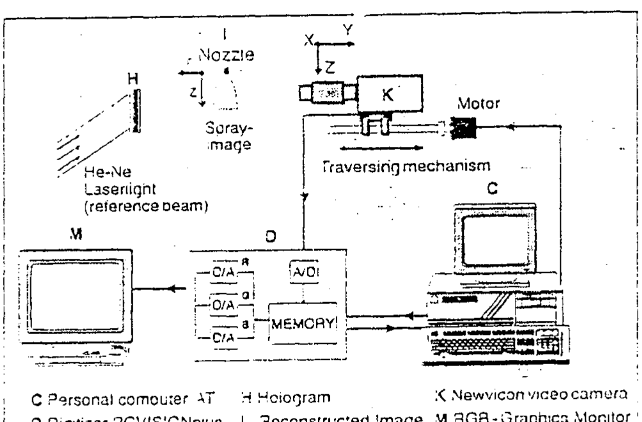

Figure 5. Digital Image-Processing System for the Evaluation of Pulsed Laser Holograms.

As mentioned before the reconstructed image is of three-dimensional extension and by using a lense of a long focus, only a very narrow area of the spray will be well focused. This has the advantage, that the spray cloud can be evaluated plane by plane, either by adjusting the focal plain of the lense or by moving the camera forward or backward with a fixed focus of the lense. The latter procedure has the benefit, that the scale of the image, recorded in the video-camera, is not changed. That is the reason why it is preferably used in technical applications.

The very rapid development of computer technology made image analysis and image-processing applicable in many technical and scientific areas. Numerous problems of pattern-recognition, data handling of digitised pictures and computer graphics - formerly only reserved for computing centres - can now be solved on a personal computer. These modern techniques can also be applied to holograms, representing pictures of conditions in two-phase flow. The purpose of digital image-processing is to reflect the main features of a picture more clearly and informatively, than in the original and to judge the contents of an image quantitatively by employing pattern recognition algorithms. In the following some principles of digital image processing for evaluating pictures of droplet fields, obtained from holographic reconstructions and the corresponding set-up of a computer aided image-processing system, is briefly described. Basic steps necessary to digitise a picture are

- superposition of a two-dimensional grid
- with a simple black and white image
- quantization of the pixels in a grid box
- transfering the pixel pattern into a binary matrix.

The quality of a digitised picture depends on the mode of digitation i.e. on the sampling and on the quantization. For very high quality it is desirable, that the width of a grid box is of the magnitude of the grain of the photographic layer. A detailed description of the numerical technique to perform the processes for grey value pictures can be found in Gonzales and Wirtz (1977) and in Pavlides (1982). A good introduction was published by Haberäcker (1987).

If the pictures, to be evaluated, are obtained from holographic reconstructions by using a video-camera, it is necessary to scan them. With the procedure of scanning we have to distinguish between in-line holograms and off-axis holograms. In the optical arrangement for recording in-line holograms the optical access of the object-beam coincides with the reference-beam. Both beams also coincide with the optical axis of the scanning camera. To resolve fine details of the object, the scanning camera can be equipped with a micro-lens, which reveals only a small fraction of the whole picture. To scan the whole object part by part, a relative movement between hologram and camera has to be facilitated. Equipments are on the market, which allow to fix a holographic plate in a traversing mechanism, movable in three dimensions.

For the reconstruction of off-axis holograms a laser-beam is used, having the same angle of incidents at the holographic plate as the reference-beam at the moment of the holographic recording. The illumination of the holographic plate by the reconstruction beam reproduces the object-beam, which contains the spatial information of the object. Also this holographic reconstruction can be scanned by a video-camera. In this case however, the only possibility to realise the relative motion between reconstructed picture and video-camera is to move the video-camera. A movement of the photo-plate would change the illumination.

The processing of images obtained from holograms involves:

- the separation of the image from the background
- the identification of sharp focused image
- parts, measuring of their projected areas and
- the evaluation of their equivalent diameters or
- center points in respect to a reference frame.

These processing steps will be explained, using the example of a dispersed two-phase flow behind an injecting nozzle. By applying an average filter, the noisy background can be suppressed. There is software on the market, which can be used to do this.

After the suppression of the noisy background, the sharply focused parts of the image - in this case droplets - have to be identified. This can be realised by contouring these parts of the image. To explain this procedure, instead of droplets more simple objects are chosen here, namely glasspearls adhered to a thin wire. Fig. 6 presents two reproductions of a hologram, taken from these glasspearls, where the first one was well focused, and the second one was 1 mm out of focus. The histograms in Fig. 6 represent the grey value along the line, which cuts the contour of the second pearl.

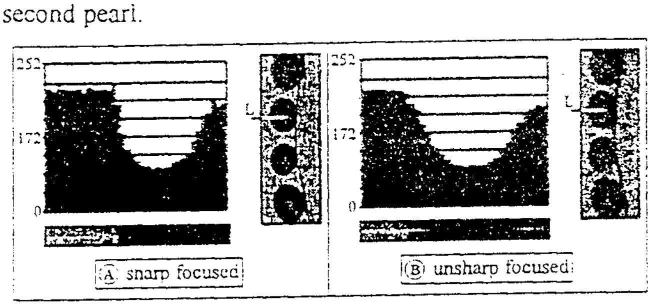

Figure 6.Histogram of Grey Value of a Sharply Focused and an Unsharply Focussed Image.

From the observation of both images and their corresponding histograms it is obvious, that sharply focused contours deliver a strong gradient of grey values and unsharply focused ones show a smooth transition of grey values. The decision about the sharpness of a contour is made by a digital image processing system. For this procedure many so called "out of focus"-algorithms have been developed and are available from literature (Ligthart and Groen 1982). Based on the different gradients of the grey values, a Sobel-operator enhances strong gradients, while making images with weak gradients disappear. The last step is to eliminate all images, which are not well focused. This can be done by allowing only pixels to remain in the image, which have a grey gradient to their neighbours above a certain value. For details reference is made to the work by Chávez and Mayinger (1992).

An example of a computerised reproduction of the veil and the droplet swarm originating from a nozzle is shown in the Fig. 7 and Fig. 8. They convey an impression of how the information of the hologram can be improved by computerised evaluation. While the photograph on the left side of Fig. 7 shows only the shape of the veil, the computerised picture on the right side clearly presents the thickness of the liquid film of the veil and also shows its wavy nature. In addition the droplets, operating from the lower end of the veil are clearly defined.

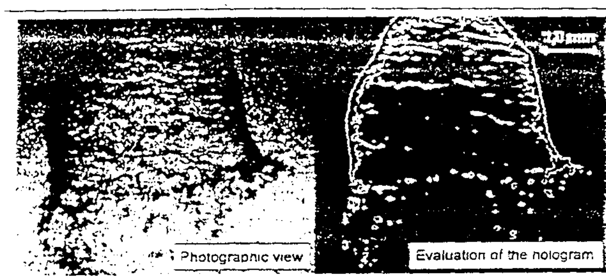

Figure 7.Veil and Spray Flow Behind a Nozzle: Photographic View and Evaluation of the Hologram.

Fig. 8 presents the sequence of reproduced "pictures" by this computer-aided image-processing. The upper row in this figure shows the region of the spray near the nozzle and the lower one, a region further downstream, where the veil is already disintegrated into a droplet swarm. By applying specially developed algorithms (Chávez 1991), the cross-section area, the diameter and the concentration of the droplets can be determined.

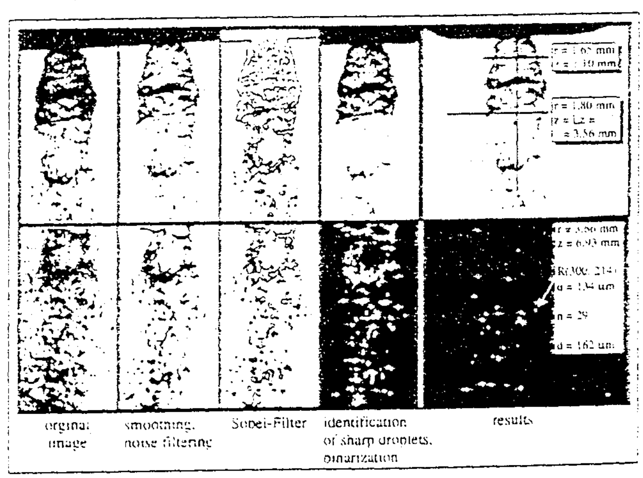

Figure 8. Steps of Image-Processing of a Hologram.
Upper Row: Spray Near the Nozzle.
Lower Row: Spray Downstream the Nozzle.

The figure gives an impression how the numerical procedure changes the original photographic picture into a computerised one, which contains only information of particles, being exactly in the focus plane, a slice, which in this case is thinner than 0.5 mm.

If two exposures of a moving particle collective are illuminated onto the same holographic plate within a short time, the velocity of the particles can be determined from such a hologram (Chávez and Mayinger 1992). For simplicity sake let us assume, that the particles are only moving in a two-dimensional way i.e. within the focused layer of the holographic reproduction.

Now a Fourier analysis is applied. To do this, the computer starts a process in which each image of the droplet is connected with all other ones and where the distance, as well as the angle with reference to the nozzle access between two "images" is determined. The Fourier analysis converts the spatial distribution into an normalised frequency distribution, as shown in Fig. 9 for the angle and for the distance of the connecting lines. The preferential angle appears as a peak in the Fourier diagram, showing the main direction and by this the direction of the movement of the particles. The same is done with the distance of the droplet "portraits". Now the preferential distance appears as a peak in the Fourier diagram. From that the average velocity can be calculated by using the time distance between the two exposures.

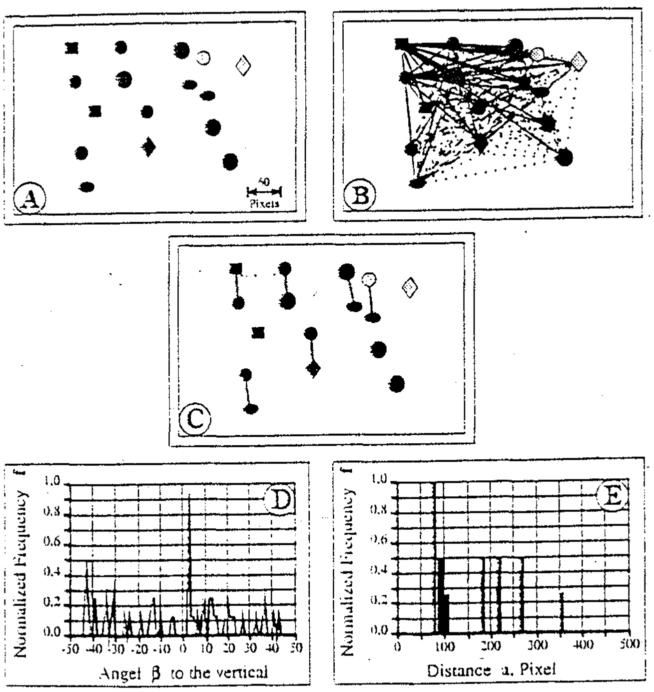

Figure 9. Steps for the Recognition of Couples of Spots. Corresponding to Two Successive Positions of Droplets.

If the movement of the particles is strongly three-dimensional, the procedure is much more complicated. In such a case electronically reproduced pictures of 3 or more focus planes have to be taken into account and the searching for the image of the second exposure of a particle has to be extended to all these planes being under consideration. So the Fourier analysis can be made in a three-dimensional way.

The results of a Fourier analysis in a two-dimensional way are presented in Fig. 10. The method is accurate enough to monitor even small influences on the droplet velocity, as they are for example produced by varying the pressure of the gas atmosphere into which the spray and by this the droplets are injected.

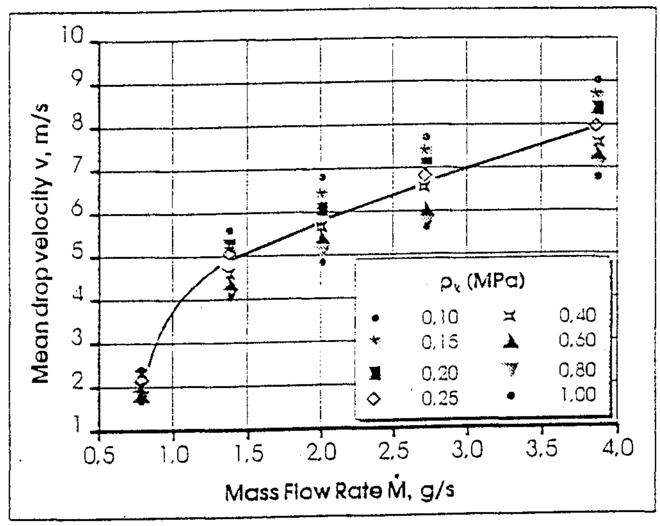

Figure 10. Mean Droplet Velocity in a Spray as a Function of the Flow-Rate at Different Ambient Pressures.

3. HOLOGRAPHIC INTERFEROMETRY

In flow boiling heat transfer, we are interested in heat flux densities, temperature fields and resulting from this in heat transfer coefficients. A very powerful method to record temperature fields and temperature gradients is the holographic interoferometry. The benefit of holographic interferometry compared to other interferometric methods - like Mach-Zehnder interferometry - is, that there is no need for a high optical quality of the optical components, because only relative changes of the object wave are recorded, and optical errors are automatically compensated by this interferometric method. On the other hand the monochromatic light, producing the wave-front, has to be very stable, therefore a laser of good coherence is needed as a light-source. There are many possibilities for arranging optical set-ups to form a holographic interferometer, which cannot be discussed here in detail. Reference is made to the literature (Mayinger 1994, Mayinger and Panknin 1974 and Panknin 1977).

A most commonly used arrangement for a holographic set-up is shown in Fig. 11. By means of a beam-splitter, the laser-beam is devided into an object and a reference-beam. Variable beam-splitters are especially useful for allowing easy adjustment of the intensities of the beams. Both beams are then expanded to parallel waves by a telescope, which consists of a microscope-lens and a collimating lens. The object wave passes through the test section, in which the temperature field is to be examined, whereas the reference wave directly falls onto the photographic plate.

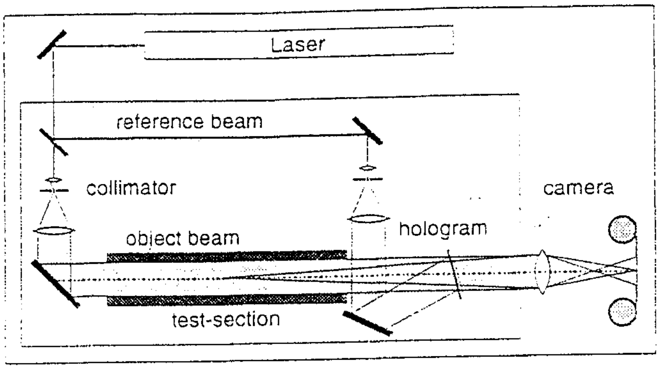

Figure 11. Optical Set-Up for Holographic Interferometry.

To obtain good reconstructions from a hologram, the inter-ference pattern between object and reference wave must be stable during the exposures of the plate. Therefore the optical components are mounted on a vibrationfree table. To avoid even those vibrations, which can be caused by water-cooled laser, it is sometimes necessary to place the laser away from the optical set-up.

The principle of the holographic interferometry is, that two waves are superimposed, which passed through the same test section at different moments. Therefore changes, which occur between the two recordings are interferometrically measured. For measuring the heat transfer for example, the recording of the first wave - the first exposure - is made, when all desired processes in the test section are in operation - fluid flow, pressure and mean temperature - but not that process - the heat transfer from an object, from a plate or from a bubble - which is of interest. There are in principle 2 techniques to record both exposures:

- the double exposure technique and
- the real time technique.

3.1 Recording Techniques for Holographic Interferometry

At first, the double exposure technique, which is very simple to use, will be briefly described. According to the holographic principle, several object waves can be recorded, one after the other on one and the same hologram. By illuminating with the reference wave, they are all simultaneously reconstructed. If they differ only slightly from one another, they will interfere micro-scopically. In the interference pattern, the differences between the object waves are discernible. This principle is used for the double exposure technique, illustrated in Fig. 12. In this illustration, the temperature distribution in a heated tube is chosen as an example. In a first exposure, the wave passing through the test section with constant temperature distribution is recorded. After recording this first exposure, the phenomena to be investigated is started. In this case, the temperature field is established by heating the wall of the tube. Now the incoming wave receives a continuous, additional phase-shift, due to the temperature changes. This resulting wave-front called the measuring-beam is recorded on the same plate. After processing, the hologram is repositioned and illuminated by the reference-beam. Now both object waves are reconstructed simultaneously and will interfere. The interference picture can be observed or photographed. The main difference from classical interferometry is, that the object-beam is compared to itself. This allows a range of new applications, improvement and simplifications of optical interferometry, compared to conventional techniques. Since both waves pass through the same test section, any imperfections on the windows, mirrors and lenses are eliminated. Examinations even at very high pressure can be made, because the deformation of the windows can be compensated.

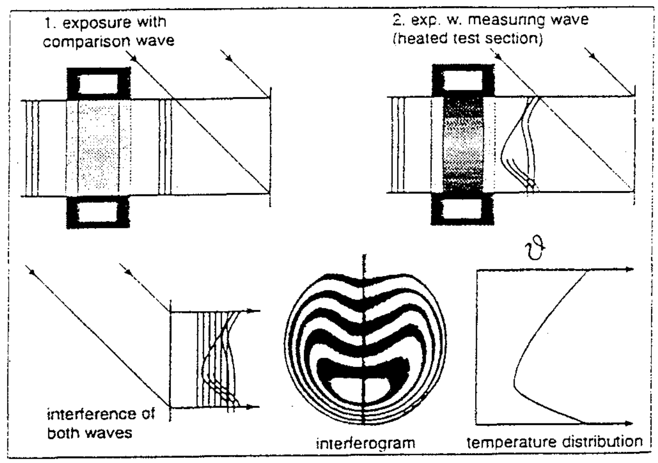

Figure 12. Principle of the Double Exposure Technique.

The method of double-exposure technique has the benefit, that it is simple to handle, however, it has the draw-back, that the experimentalist does not see, what he has recorded until the photographic plate is chemically processed, which usually takes 1/2 an hour. With the double-exposure technique, the investigated process cannot be continuously recorded, which is another disadvantage. Therefore a more sophisticated recording process for holographic interferometry was developed, the so-called real-time-method, which is illustrated in Fig. 13.

After the first exposure, by which the comparison wave is recorded and during which no heat transfer is going on in the test section, the hologram is developed and fixed. After this chemical process, the photographic plate is repositioned accurately to its old place, and the comparison wave can be reconstructed continuously by illuminating the photographic plate - the hologram - with the reference wave. This reconstructed wave, showing the situation without heat transfer in the test section, can now be superimposed onto the momentary object wave. If the object wave is not changed, compared to the situation before the chemical developing process, and if the hologram is precisely repositioned, no interference fringes will be seen on the hologram.

This indicator can be used for replacing the hologram exactly to its old place - within an accuracy of half a wavelength - by using micrometer and piezo quartz positioning devices.

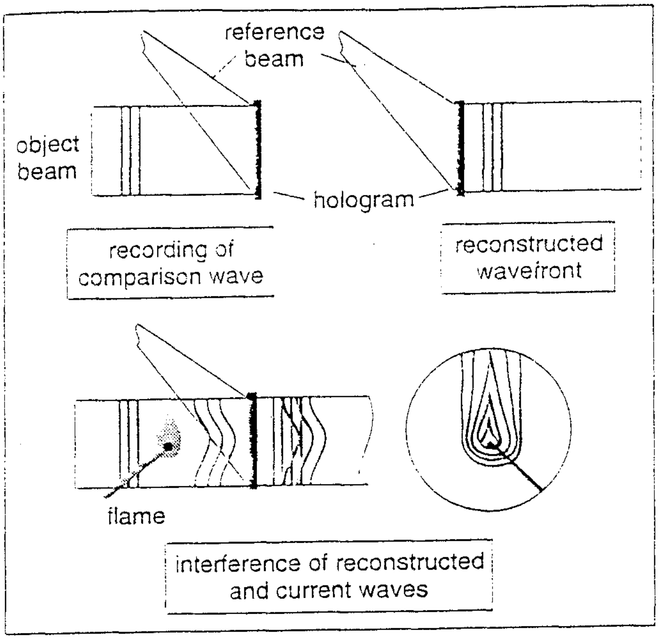

Figure 13. Principle of the Real-Time-Method.

After repositioning, the heat transfer process can be started. Due to the heat transport, a temperature field is formed in the fluid, and the object wave receives an additional phase-shift, when passing through this temperature field. Behind the hologram, both waves interfere with each other, and the changes of the interference pattern can be continuously observed or photographed.

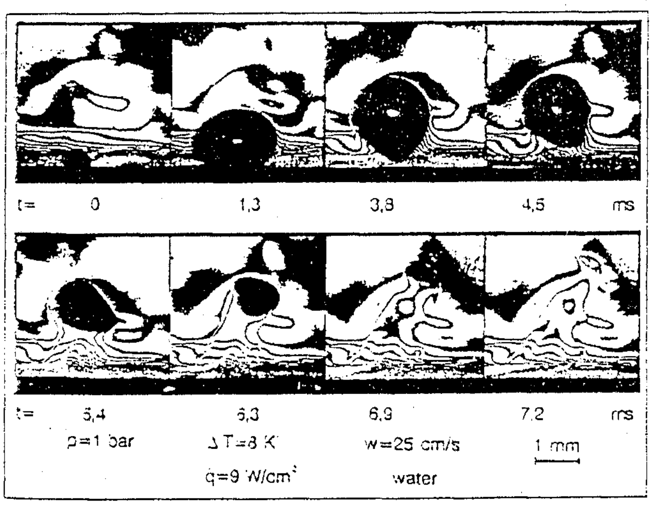

Figure 14. Detachment of a Single Bubble from a Heated Wall.

An example of such an holographic interferogram shows Fig. 14, which was taken from a simple flow boiling process. Slightly subcooled water was slowly flowing over a horizontal surface, which was electrically heated. Due to the heating, nucleation started in the superheated boundary layer and a bubble was forming. In the first sequences of the interferograms, shown in Fig. 14, the bubble gets heat and by this also mass from the superheated boundary layer, and it grows rapidly in a few milliseconds. The black and white lines - called fringes - in these interferograms represent in a first approximation isotherms in the liquid, and the temperature difference between each isotherm is constant, as explained a little later. So one can read the fringes like a pattern of constant height - in this case temperature height - and, where the fringes are close together, there is a steep temperature gradient, and where they are far apart, a plateaux of almost constant temperature - small gradients - is demonstrated.

In Fig. 14 one can also see the limitation of this method, which is due to the fact, that the light, passing through the heated test section is not only shifted in phase, but is also deflected. So depending on the sign of the temperature gradient - positive or negative - the laser-beam is deflected either to the wall or from the wall. Therefore in a thin zone very near to the wall, we get no information and we can only see a grey pattern without interference fringes.

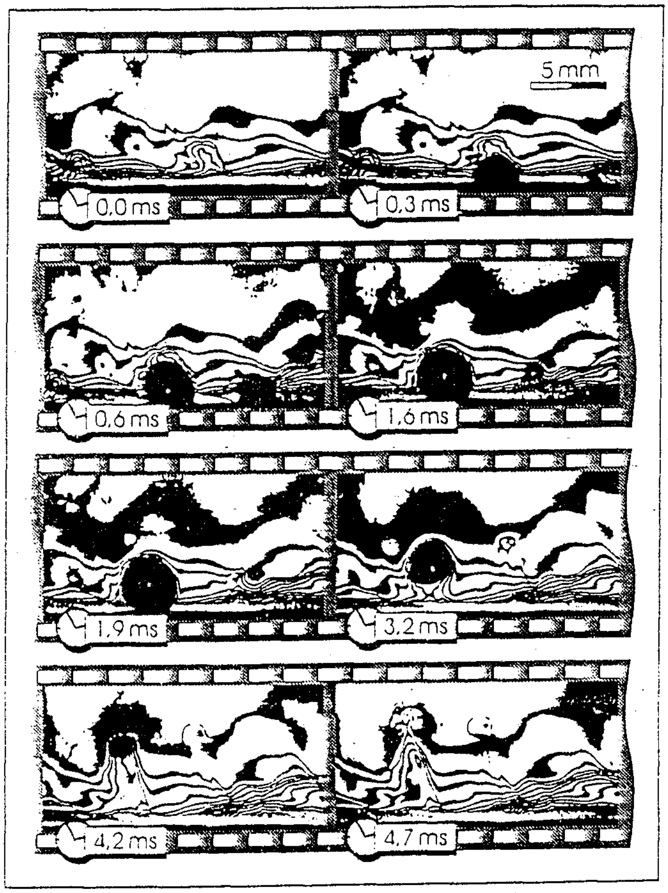

Figure 15. Detachment and Recondensation of Bubbles Under Various Boundary Conditions.

Following the sequences, presented in Fig. 14, we realise, that the vapour bubble, after penetrating from the superheated and saturated layer near the wall into the subcooled bulk of the liquid, starts to condense again and disappears within approximately 7 ms. The boundary layer is highly inhomogenous and is disturbed by the growing and by the buoyancy induced rising of the bubble.

Boiling on a heated surface is a statistical process and nucleation as well as recondensation of a forming bubble can not at all be described by a simple theory. This is demonstrated in Fig. 15. There also a sequence of interferograms is presented, covering a total time span of approximately 5 ms. Under a relatively thick boundary layer with flat temperature distribution, a bubble starts to form (0,3 ms), grows and recondenses again after reaching the subcooled bulk of the fluid, which in this case is also water. Bubble growth and recondensation is finished after 4,7 ms.

Another bubble also at the moment of 0,3 ms starts to grow under a position of the boundary layer with high temperature gradient. Due to the high temperature gradient, this bubble grows explosively within 0,3 ms, moves very fast into the subcooled bulk and condenses there as rapidly as it was grown. Its total lifespan is less than a half of that of the first bubble. For getting quantitative data of the temperature distribution and also for derivating the heat transfer coefficient, we have to perform an evaluation procedure according to the optical laws. This evaluation procedure will be briefly described in the following:

3.2 Evaluation of the Interferograms

The evaluation of a holographic interferogram, made in an optical set-up with parallel object wave, is very similar to the evaluation of interference patterns recorded in a Mach-Zehnder interferometer (Mayinger 1994, Mayinger, Panknin 1974). Therefore only the basic equations will be given. In Mach-Zehnder interferometry the wavefront, which is distorted by the object in the test section, is compared to a plane wave. In holography the object waves, passing through the test section at different times are superposed, and therefore reveal the changes in optical pathlength between the two exposures. Expressed in multiples S of a wavelength, this change is calculated to

$$S(x,y)\cdot l = l\left[n(x,y)_2 - n(x,y)_1\right] \qquad (1)$$

l is the length of the test section, in which the refractive index is varied, because of temperature or concentration changes. The refractive index distribution n(x,y) during the recording of the two waves is assumed to be two-dimensional (no variation in light direction). Equation (1) shows, that initially only local variations can be determined. Only if the distribution of the refractive index n $(x,y)_1$ during the recording of the comparison wave is known, absolute values can be obtained. Therefore one usually establishes a constant refractive index field (constant temperature) while recording the comparison wave.

$$S(x,y)\cdot\lambda = l\left[n(x,y)_2 - n_\infty\right] \qquad (2)$$

To obtain absolute values for the temperature field, the temperature at one point of the cross section has to be determined by thermocouple measurements. This is usually done in the undisturbed region or at the wall of the test chamber. Equation (2) is the equation of ideal interferometry. It was assumed, that the light ray propagated in a straight line. Passing through a boundary layer, the light rays, however, are deflected because of refractive index gradients.

The light deflection can be converted into an additional phase shift ΔS, if a linear distribution of the refractive index is assumed to be within this small area.

$$\Delta S = \frac{n_0\cdot\lambda\cdot l}{12\cdot b^2} \qquad (3)$$

b is the fringe width, n_0 the average refractive index.

In many applications an ideal two dimensional field cannot be found. Often the boundary layer extends over the ends of the heated wall, or there are entrance effects or temperature variations along the path of the light beam (axial flow in the test section). Therefore only integrate values are obtained. Having corrected the interferogram, the obtained refractive index field can be converted into a density field. The relation is given by the Lorentz-Lorenz-formula, where N is the molar refractivity and M the molecular weight.

$$\frac{n^2-1}{n^2+2}\frac{1}{\rho} = \frac{N}{M} \qquad (4)$$

For gases with n=1, this reduces quite accurately to the Gladstone-Dale-equation.

$$\frac{2}{3}(n-1)\frac{1}{\rho} = \frac{N}{M} \qquad (5)$$

If there is only one component in the test section, and the pressure is kept constant, the density variations can only be caused by temperature changes. If the fluid is a gas, one can use the equation of state, in order to obtain the following formula, which relates the fringe shift to the temperature.

$$T(x,y) = \left[\frac{S(x,y)\ 2\cdot\lambda\cdot R}{3\ N\cdot p\cdot l} + \frac{1}{T_\infty}\right]^{-1} \qquad (6)$$

For liquids, the situation is more complicated. One has to go back to equation (1) or equation (2) respectively, and one has to use an equation from the literature, which correlates the refractive index with the temperature, being available in handbooks from thermodynamics.

Often local heat transfer coefficients are of special interest. In this case the temperature gradient at the wall is determined, and assuming a laminar boundary layer next to the wall, the heat transfer coefficient is obtained by :

$$\alpha = \frac{-k \cdot \left(\frac{dT}{dy}\right)_w}{T_w - T_\infty} \qquad (7)$$

3.3 Finite Fringe Method

With very high heat transfer coefficients, the boundary layer at a heat-transferring surface becomes very thin, down to a few hundreds of a millimetre. In this case it is difficult to evaluate the interference pattern, if it is registered with the procedure, described up to now. A slightly altered method, the so called "finite fringe method" offers some benefits. In this method, after the reference hologram was produced, a pattern of parallel interference fringes is created by tilting the mirror in the reference wave of Fig. 16, or by moving the holographic plate there within a few wave-lengths. The direction of the pattern can be selected as one likes, and it only depends on the direction of the movement of the mirror or of the holographic plate. By imposing a temperature field, due to the heat transport process, this pattern of the parallel interference fringes is then distorted. The distortion or deflection of each fringe from its original parallel direction is a measure for the temperature gradient at this spot and allows to deduce the heat flux and by this the heat transfer coefficient.

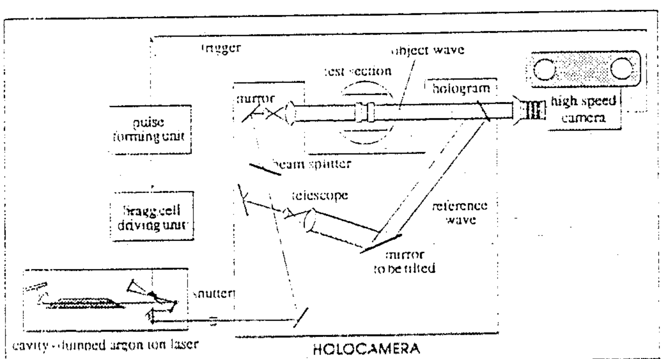

Figure 16. Finite Fringe Method for Holographic Interferometry.

In Fig. 17 this method is applied for monitoring the boundary layer and by this also the heat transfer at the phase interface at a bubble, filled with saturated vapour and condensing in a subcooled liquid of the same substance. The velocity of the condensation and by this the movement of the phase interface can be controlled by the heat transfer process or by inertia forces. The left interferogram in Fig. 17 demonstrates the situation at the phase-interface between vapour and liquid, when the heat transfer dominates and the right one gives an impression of inertia controlled condensation. In the latter case, the heat transfer coefficient cannot be measured by the holographic interferometry, because there is no laminar boundary layer at the phase interface.

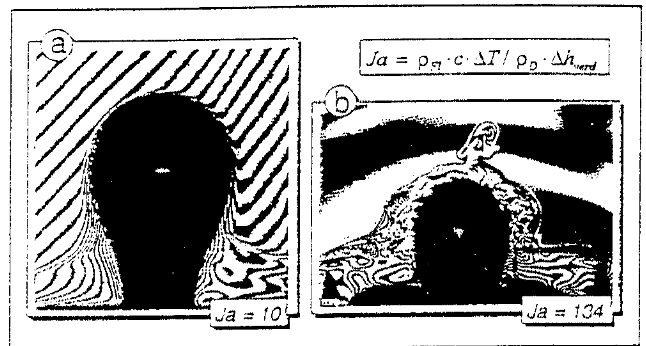

Figure 17. Phase Interface Boundary Layers with Heat Transfer- and Inertia Controlled Condensation.

The interferogram on the left-hand side has to be interpreted in such a way, that in these areas, where the interference fringes have a constant gradient (parallel lines), resulting from tilting the mirror or moving the holographic plate, there is a homogeneous temperature field. When the temperature changes, due to heat transfer, these parallel lines are deflected and the change in the original direction - the deflection of the fringe - can be used for evaluating the local and instantaneous heat transfer coefficient. For details of this evaluation process, reference is made to the literature (Nordmann, Mayinger 1981 and Chen, Nordmann, Mayinger 1991).

A sequence of evaluations of such interferograms is presented in Fig. 18. The sequence of these interferograms was taken by combining the holographic interferometry with the high-speed cinematography. The method allows instantaneous and local measurements of the heat transfer coefficient with good accuracy.

Saturated steam was blown through a capillary into slightly subcooled water. A bubble is formed at the outlet of the capillary and the condensation process starts immediately. For a short period - approximately 15 ms - the condensation at the phase interface reduces the volume of the bubble to a larger extent, than steam can be fed into the bubble via the flow through the capillary. Therefore in the scene 2 (approximately 10 ms after the opticalmonitoring started) the bubble takes a "squatting position" and the heat transfer at the top of the bubble is strongly reduced by the moving down of the layer of saturated liquid formed before and now insulating the steam from the subcooled bulk. Afterwards the steam flow through the capillary can overcome the rate of the condensed volume again, the bubble grows, separates from the nozzle and the heat transfer coefficient is increased.

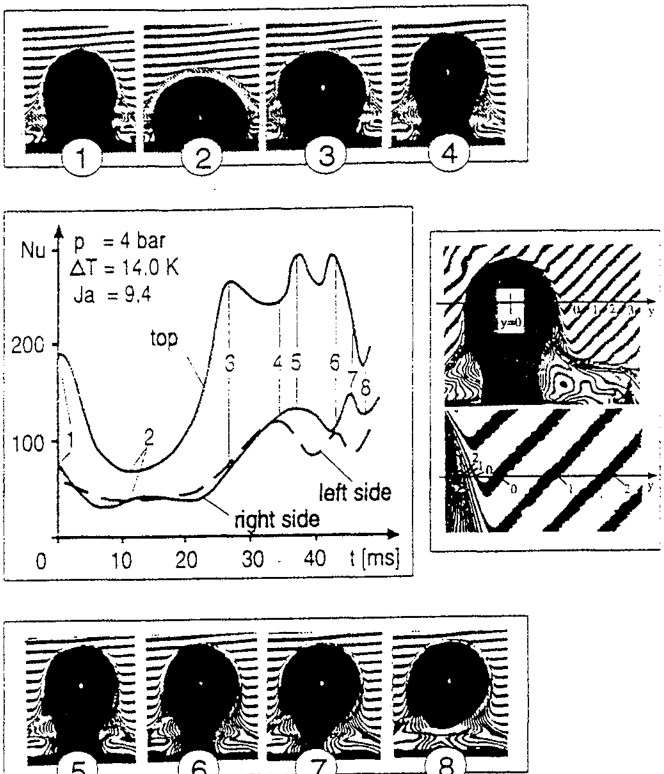

Figure 18. Heat Transfer at the Phase-Interface of a Vapour Bubble, Condensing in a Subcooled Liquid, Deduced from a Sequence of Interferograms.

4. LASER-INDUCED FLUORESCENCE

Light as sensor can provide several informations and not only the refractive index and the phase-shift can be used to get information about the distribution of temperature in a substance or of concentration in a mixture. Besides the phase-shift, the effect of scattering is most commonly used to get information about the physical and chemical conditions in a liquid or in a gas. Scattering methods are for example

- Raman-scattering
- Rayleigh-scattering
- Mie-scattering
- Bragg-scattering or
- Brillouin-scattering

It should be briefly mentioned, that Mie-scattering is recently used for flow visualisation in the particle-image-velocimetry (PIV). For using this method, a laser beam is formed into a very thin light-sheet, illuminating a plane within the volume of interest. For one measurement, 2 consecutive laser pulses are fired within a very short time interval, and the radiation, scattered by the particles in the illuminated area, is recorded two-dimensionally by a camera. The diameter of scattering particles usually is between 3 µm and 300 µm.

Here only the laser-induced fluorescence will be discussed a little more in detail. When applying this method, the molecule under consideration absorbs one photon of the incoming laser-light. The energy of the photon must be equal to the energetic difference of two energy levels, i.e. the original level in the ground electronic state and a corresponding level in the first electronic state. The situation is principally explained in Fig. 19.

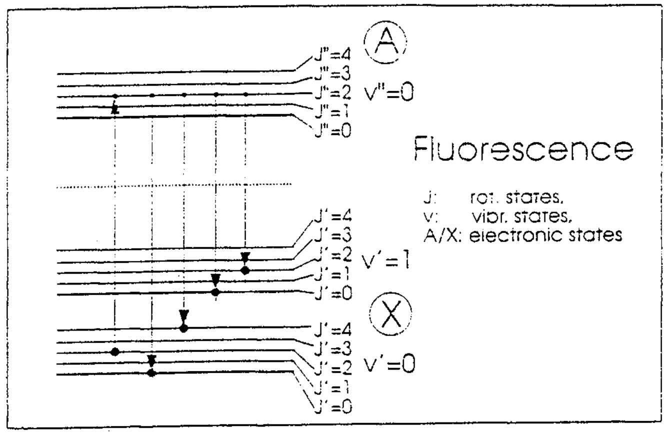

Figure 19. Energy Diagrams for Laser-Induced Fluorescence.

Since the energy differences involved are discrete and specific for each species, the frequency of the laser light has to be chosen in accordance with the molecule of interest. The states in the upper electronic levels are semi-stable with extremely short life-times and, therefore, soon after the transition to the upper state, the excited molecule drops back to the stable energy level within the ground electronic state, emitting a photon. In the most common case, the mean part of the fluorescence occurs at the same wave-length as the incoming light. Therefore it is sometimes difficult to distinguish between primary (incoming) radiation and the radiation by fluorescence.

In competition to this laser-induced fluorescence (LIF) a somewhat revised method was developed, the so called laser-induced predissociated fluorescence (LIPF). Here the excitation transition is chosen such, that predissociation at the upper state occurs at a high rate, and the wave-length of the fluorescent light is different from that of the incoming light for one and the same molecule. A good overview and detailed information about the before mentioned fluorescence technique can be obtained from the literature (e.g. Andresen 1988/1990/1991, Hanson 1990).

LIF and LIPF can be used to measure local concentrations, especially in chemical reactions, but also in newer times, it is applied to evaporation processes. An arrangement of optical components for performing LIF or LIPF measurements is shown exemplary in Fig. 20. A laser-beam electronically excites the molecules of interest. The author of the present paper was studying the concentration fields in combustion processes by LIF (Haibel, Mayinger, Strube 1993). Fig. 20 demonstrates how the laser-beam, originating from an EXCIMER-laser is expanded and deformed into a thin light-sheet with a height of approximately 5 cm and a thickness less than 0,7 mm. This light-sheet travels through a narrow quartz-window into the reaction zone, where the fluorescence is produced. The fluorescense is observed and recorded in perpendicular direction to this light-sheet with the aid of a CCD-camera, which is in this case intensified in the same wave-length as the laser produces (308 nm). The video signal of the camera is processed in a image evaluating unit and transformed into pseudo-colour pictures. These pictures are recorded by a SVHS-video-recorder, working in an analog way. The timewise co-ordination of laser and camera is done via a triggering unit, which is synchronised by the video-camera.

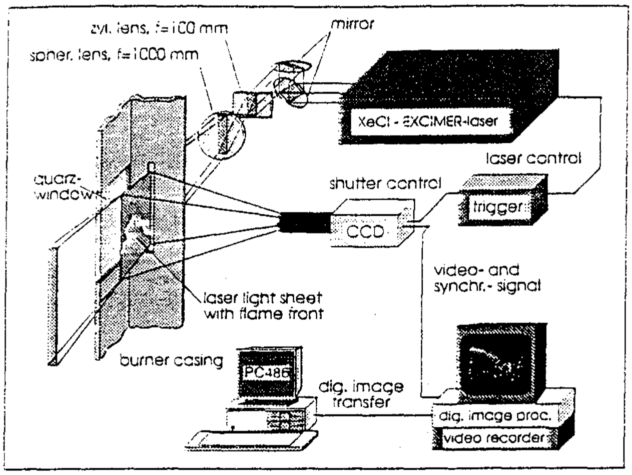

Figure 20. Optical Set-Up for Laser-Induced Fluorescence.

The chemical reaction in a flame is much more unstable and dynamic, than one would estimate by looking to the flame with the naked eye. This is also true for steady state combustion chambers. If we monitor a hydrogen flame in a simple combustion chamber, as shown in the upper picture of Fig. 21, without using the ultra-short time registration technique, we see a flame, corresponding to our usual imagination. This upper fluorescence picture in Fig. 21 integrates 50 single shots, ave-raging the distribution of the OH-radical fluorescent due to the excitation by the laser-sheet. Due to the fact, that the OH-radical is the most active product in the reaction-genetics of hydrogen combustion, the grey tunes in this figure mediate the local reaction activity. One realises zones of high reaction rates - black and dark grey areas - downstream and a little upwards of the spot where the mixture of hydrogen and air is injected into the combustion chamber.

The apparently quiet picture of the flame changes drastically, if the recording time is reduced to very short periods - down to 17 ns. Two ultrashort shots of the flame situation are shown in the lower pictures of Fig. 21. In the upper one of these two pictures, the flame is separating from the injection spot of the burner and inspite of a homogeneous mixture of hydrogen and air, there is no reaction at this spot for that moment. Such non-reacting zones can be observed - as shown in the lowest picture of Fig. 21 - over a long flowpath of the flame.

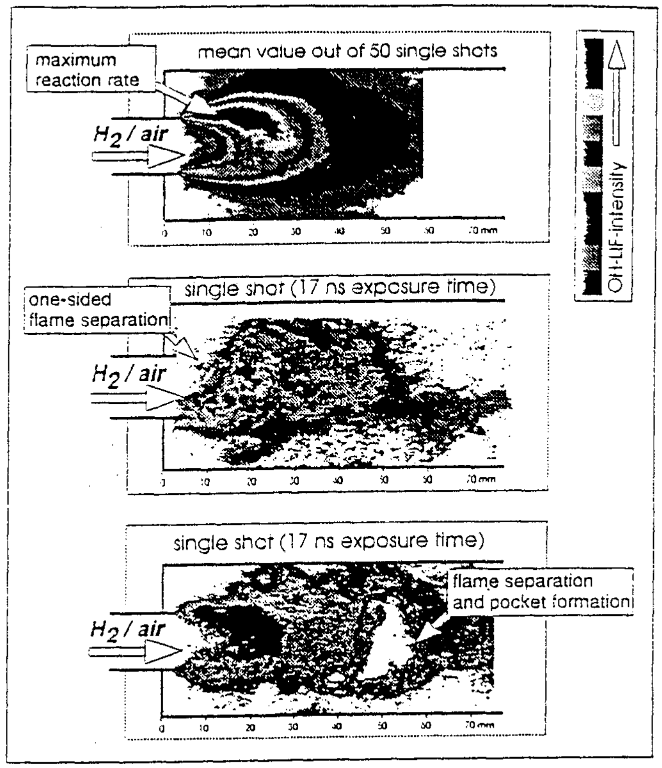

Figure 21. Structure of Premixed Hydrogen Flames in a Burner.

There are several papers in the literature, describing the use of laser-induced fluorescence for measuring vapourisation dynamics (Bazile, Stepowski, 1994, Senda, Fukami, Tanabe, Fujimoto, 1992 and Melton, Verdieck, 1985). Most of these authors use the exciplex fluorescence method.

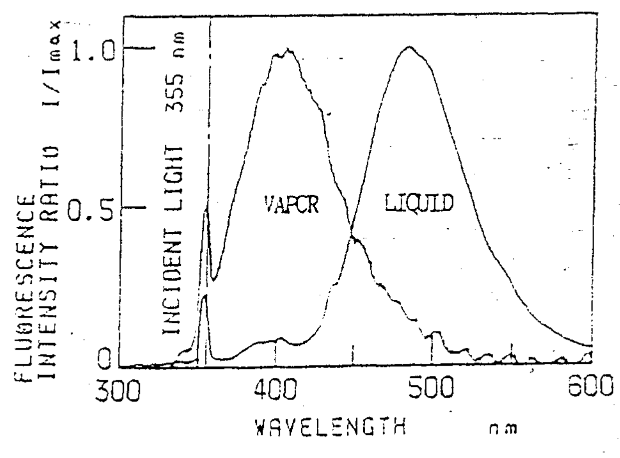

Figure 22. Frequence Spectra in Vapour and Liquid with Laser-Induced Fluorescence (Senda et al).

In this method, liquid additives - tracers are doped into the liquid to be evaporated and are assumed to be co-evaporative with it. In addition a second tracer can be added to the liquid in a very low concentration, which is not evaporating. So 2 spectra can be observed in the vapour-liquid mixture. One, which results from the fluorescense in the vapour and another one, originating from the fluorescence in the liquid. Bazile and Stepowski 1994 used the organic dye Rhodamin 6G, which does not vapourise for visualising a liquid/fuel spray. Senda e.a. 1992 reports on the visualisation of evaporative diesel spray by the excipiex fluorescence method. A TMPD monomer is used as a tracer for visualising the vapour phase. Fig. 22, taken from a paper by Senda e.a. (1992), shows fluorescence spectra of a liquid and a vapour phase. The spectra were measured by a multi-channel analyser.

5. A NOVEL IMPEDANCE METHOD

Impedance methods are widely applied for measuring the volumetric concentrations in multi-phase flows. They are based on different electrical properties (permittivity and conductivity) of the flow components and their effect on the measured impedance (capacitance and conductance) of an appropriate sensor. Although the impedance method offers a number of advantages, like instantaneous answers, its sensitivity to the flow pattern sometimes limits the range of application. Many different electrode designs have been developed, trying to minimise this limitation. Widely used arrangements are parallel plate electrodes (Auracher 1985), ring electrodes (Özgü 1973) or helical electrodes (Geraets 1988). For the generally occurring flow conditions, a number of analytical formulae are known, which connect the permittivity ε of a mixture of two fluids with their volumetric concentration ratio. These models are based on general conditions, regarding the shape of the dispersed particles and are often limited to relatively small maximum concentrations. The most popular models are those by Maxwell. The sensitivity of the impedance to the distribution pattern of the components - liquid and vapour - within the sensor leads to different calibration curves for each flow regime. In many practical flow situations, these curves differ very much.

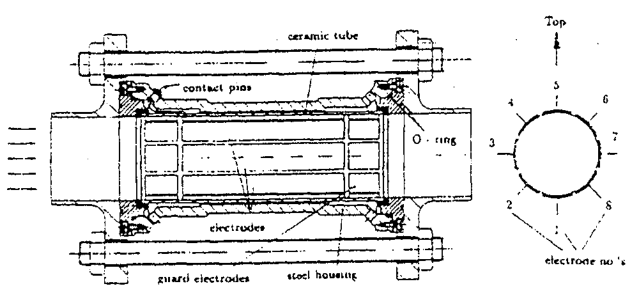

Figure 23. Impedance Sensor for Void Measurements.

To overcome the insufficiencies mentioned above, a new approach is made for measuring void fraction and flow pattern in multi-phase flows (Klug, Mayinge: 1994/1992). A non-intrusive impedance probe, consistinç of eight surface-plate electrodes implemented into the inner side of a tube (see Fig. 23).

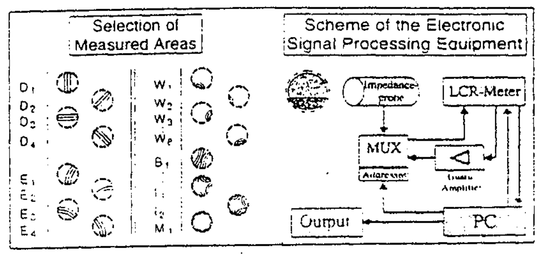

Figure 24. Examples of Measuring Fields.

With this probe, the impedance between differen combinations of electrodes - the so called measuring field: - is measured, as demonstrated in Fig. 24 For every meas uring field, the impedance - as an integral parameter - i: determined by the distribution of the phases within th whole sensing volume of the probe. However, the indi vidual domains of the sensing volume make different con tributions to the total amount of the flow-influenced prob impedance. Therefore characteristic contribution pattern for the spatial sensitivity (Bair, Oakley 1992) can be ob served, which allows to classify the multitude of measurin; fields into several groups. Each group consists of a certai: number of fields, which depends on the degree of fiel symmetry. One can distinguish between diametrical fielc (D), eccentric fields (E), wall fields (W), large fields (B integral fields (I) and Maltese-cross-shaped fields (M). Fc each field and for each flow pattern, one can make a thec retical calculation, and one can compare the theoretica prediction with the measured one. This comparison is kind of calibration.

For practical use, where the flow pattern and also th void fraction are unknown, one can switch through a these mentioned field types and by comparing the mea: ured signals with the calibration data, one finds a min mum of deviation for a certain field group and a certai flow pattern between actual measured data and calibratic values. From that, one knows which flow pattern exis during the actual measurement, and one can choose th right correlation for evaluating the impedance signals t get the local volumetric void fraction.

This method is briefly sketched in Fig. 25 for 3 di ferent flow patterns, namely stratified flow, annular flo and inversed annular flow (vapour outside and liquid in th bulk). The good performance of this reconstruction tec nique for the flow regimes, stratified flow, bubble flow ar annular flow is shown in Fig. 26. For each example, t different measuring fields are indicated, which were use to reconstruct the data.

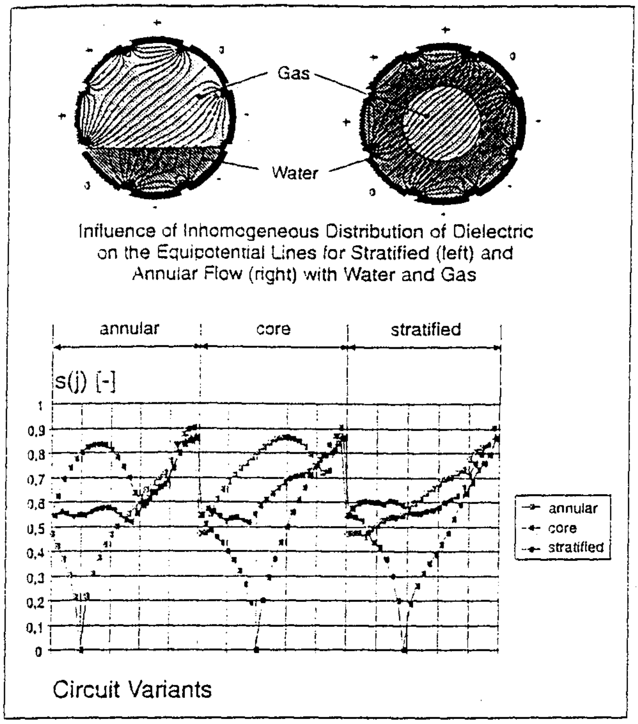

Figure 25. Calculated Derivations for 3 Cases, by Using 27 Measuring Fields.

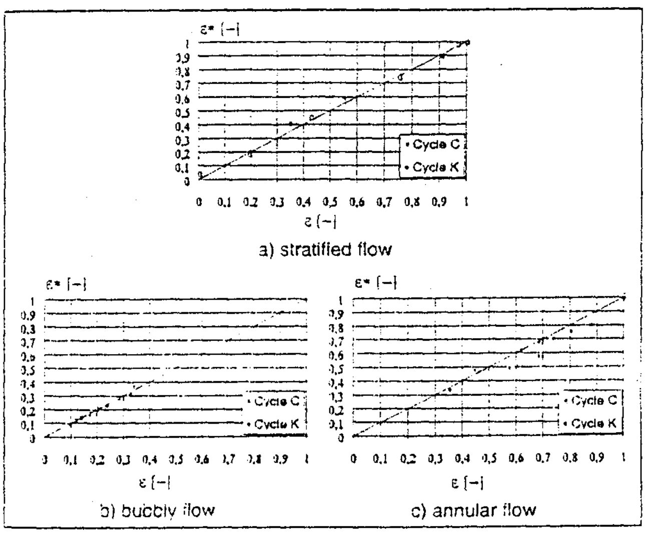

Figure 26. Calibration Tests with Impedance Sensor.

Finally in Fig. 27 a practical application of this method is presented. Three impedance probes were installed in a 2 m long pipe, through which a nonsteady, two-phase flow mixture was flowing during a blow-down process. A pressure vessel, filled partially with propane, was depressurised, feeding a liquid-vapour-mixture - due to flashing - into the pipe and flowing, via an orifice into a low pressure chamber. In the upper part of Fig. 27, the temporal course of the pressure at various positions along the pipe is shown. The lower part of this figure demonstrates clearly, that the impedance probe accurately monitors the instantaneous void fraction of the vapour-liquid-mixture at these positions.

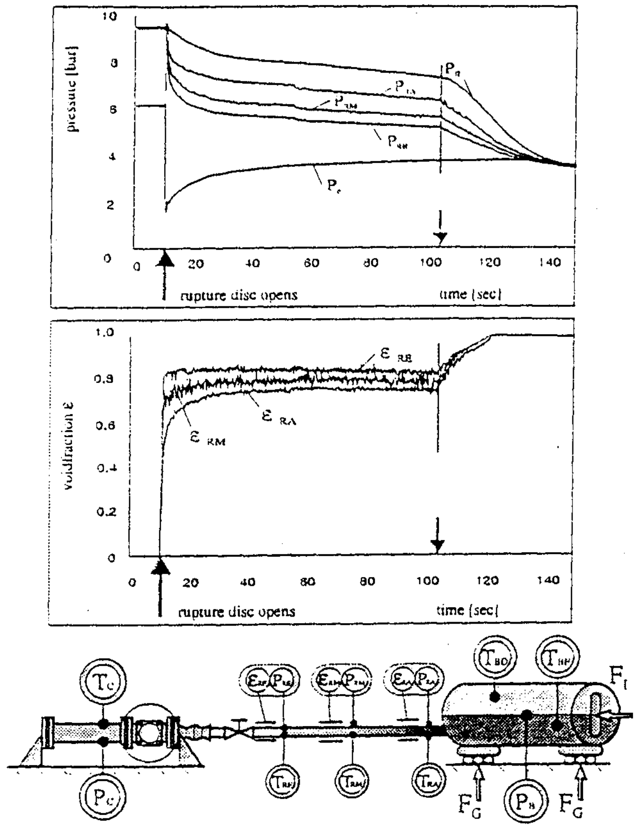

Figure 27. Pressure- and Void Distribution in a Pipe During Blow-Down.

Of course the same result would have been also obtainable by using a tomographic method, instead of the calibration procedure. However, the data handling with the tomographic method is much more time consuming, than that of the described procedure.

6. CONCLUDING REMARKS

Optical methods and also other instantaneous and non-invasive techniques are expected to experience a powerful revival, due to three reasons:

Sophisticated theoretical treatment of heat transfer with phase change and two-phase flow with large computer codes needs very detailed information about temperature distribution and flow pattern for assessing and improving the physical models, used in the codes and for verifying such codes. An optically determined pattern of isotherms and an non-invasive impedance based measurement of flow pattern is a very stringent touchstone for the reliability and accuracy of a code.

Modern developments in power- and process engineering make transient situations more and more interesting, especially for controlling procedures and safety deliberations. Non-invasive and inertialess measuring techniques are a great help for getting good informations.

A former drawback of the image forming, optical measuring techniques and for the non-invasive impedance techniques, namely the laborious and time-consuming evaluation does not exist any more. Even a personal computer is good enough for evaluating a hologram or an interferogram within a few seconds, a process, that took several hours in the past. The costs of such an evaluating equipment are relatively moderate.

A new symbiosis could come into being between theorists and experimentalists, working in heat transfer and in multi-phase flow.

REFERENCES

Andresen, P., Bath, A., Gröger, W., Lülf, H.W., Meijer, G., ter Meulen, J.J., 1988, Laser-Induced Fluorescence with tunable Laser as a possible method for instantaneous temperature field measurements at high pressures: Check with an athmospheric flame, Appl. Optics. 27: 365, 1988.

Andresen, P., Meijer, G., Schlüter, H., Voges, H., Koch, A., Hentschel, W., Oppermann, W., Rothe, E., (1990), Fluorescence imaging inside an internal combustion engine using tunable eximer lasers, Appl. Optics. 29:2392, June 1990.

Andresen, P., Wolff, D., G., Schlüter, H., Voges, H., Koch, A., Hentschel, W., Oppermann, W., Rothe, E., (1990), Identification and imaging of OH and O_2 in an automobile engine using a tunable KrF eximer laser, Appl. Optics, 1991.

Auracher, H., and Daubert, J., 2nd Int. Conf. on Multi-Phase Flow, London, 1985.

Bair, M.S., and Oakley, J.P., 1st Meeting European Concerted Action on Process Tomography, Manchester, March 26-29, 1992 (1992).

Bazile, R., Stepowski, D., Measurements of the vapourisation dynamics in the development zone of a burning spray by planar laser-induced fluorescence and Raman scattering, Experiments in Fluids 16,171-180 (1994).

Chàvez, A., Holografische Untersuchung an Einspritzstrahlen - Fluiddynamik und Wärmeübergang durch Kondensation, Diss. Techn. Univ. München 1991.

Chàvez, A., Mayinger, F., (1992), Measurement of direct-contact condensation of pure saturated vapour on a injection spray by applying pulsed laser holography, Int. J. Heat Mass Transfer, Vol. 35 No. 3, pp 691-702, 1992.

Chen, Y.M., Mayinger, F., Nordmann, D., Heat Transfer at the phase-interface phenomena in Multiphase Flow. Eds.: Hewitt, G.F., et al. New York: Hemisphere, 1991, S.433-442.

Gabor, D., A New Microscopic Principle, Nature 161, 777 (1948). Microscopy by Reconstructed Wavefronts, Proc. Roy. Soc. A 197, 454 (1949). Microscopy by Reconstructed Wavefronts II, Proc. Phys. Soc. B 64, 449 (1951).

Geraets, J.M., and J.C. Int. J. Multiphase flow 14, No. 3 (1988) 305-320.

Gonzales, R.C., Wintz, P. (1977), Digital ima[illegible] processing, Addisson-Wesley, Massachussetts.

Haibel, M., Mayinger, F., Strube, G., Application [illegible] non-intrusive diagnostic methods to sub- and superson[illegible] H_2-air combustion, 3rd intl. Symposium on special topi[illegible] in chemical propulsion: non-intrusive combustion dia[illegible]nostics, Scheveningen, NL, 1993.

Hanson, R.K., Seitzmann, J.M., Paul, P.H. (1990) Planar fluorescence imaging of combustion gases, Applie[illegible] Physics, Vol. B. 50.

Kiemle, H. and Röss, D., Einführung in die Techni[illegible] der Holographie, Akademische Verlagsgesellschaft, Frank-furt a.M. (1969).

Klug, F. and Mayinger, F., Proc. NURETH-5 Meeting Salt Lake City, Sept. 21-24, 1992 (1992).

Klug, F., Mayinger, F., Impedance based flow recon-struction - A novel flow composition measuring techniqu[illegible] for multi-phase-flows, Nuclear Engineering and Design 146, 35-42 (1994).

Lighthart, G., Greon, C. (1982), A Comparison of dif-ferent autofocus algorithms, IEEE Transactions, Vol. XX pp 597-604.

Mayinger, F., Optical Measurements, Techniques an[illegible] Application, Springer Verlag, Heidelberg, (1994).

Melton, L.A. and Verdieck, J.F., Vapour/Liqui[illegible] Visualisation for Fuel Sprays, Combust. Sci. and Tech., 42, 217-222, (1985).

Nordmann, D. and Mayinger, F., Temperatur, Druck und Wärmetransport in der Umgebung kondensierender Blasen, VDI-Forschungsheft 605, 1981.

Özgü, M.R. and Chen, J.C., Rev. Sci. Instrum. 44, No. 12, (1973), 1714-1716.

Panknin, W., Mayinger, F., (1974), Holography in Heat and Mass Transfer, 5th Int. Heat Transfer Conference, VI, 28, Tokio.

Panknin, W., (1977), Eine holographische Zweiwellenlängen Interferometrie zur Messung überlagerter Temperatur- und Konzentrationsgrenzschichten, Diss. Universität Hannover.

Panknin, W., Mayinger, F., (1978), Anwendung der holographischen Zweiwellenlängen Interferometrie zur Messung überlagerter Temperatur- und Konzentrationsgrenzschichten, Verfahrenstechnik, Vol 12, No. 9, pp 582-589.

Pavlidis, T., (1982), Algorithms for graphics and image processing, Springer Verlag, Berlin.

Senda, J., Fukami, Y., Tanabe, Y., Fujimoto, H., Vizualization of Evaporative Diesel Spray Impinging Upon Wall Surface by Exciplex Fluorescence Method, Proc. of the Int. Congress and Exposition, Detroit, February 24-28, 1992, SAE.